Received: 8 February 2019 | Revised: 24 September 2019 | Accepted: 25 September 2019

DOI: 10.1111/geb.13022

RESEARCH PAPER

Global Ecology and Biogeography A Journal of Macroecology WILEY

Defining isoscapes in the Northeast Pacific as an index of ocean productivity

Boris Espinasse[1,2] | Brian P. V. Hunt[1,2,3] | Sonia D. Batten[4] | Evgeny A. Pakhomov[1,2,3]

[1]Department of Earth, Ocean and Atmospheric Sciences, University of British Columbia, Vancouver, British Columbia, Canada

[2]AERL, Institute for the Oceans and Fisheries, University of British Columbia, Vancouver, British Columbia, Canada

[3]Hakai Institute, Heriot Bay, British Columbia, Canada

[4]CPR Survey, Marine Biological Association UK, Nanaimo, British Columbia, Canada

Correspondence
Boris Espinasse, AERL, Institute for the Oceans and Fisheries, University of British Columbia, 2202 Main Mall, Vancouver, BC, Canada V6T 1Z4.
Email: boris.espinasse@laposte.net

Funding information
G. Unger Vetlesen Foundation

Editor: Derek Tittensor

Abstract

Aim: We modelled isoscapes in the Northeast (NE) Pacific using satellite-based data, with the main objective of testing whether isoscapes defined by a few key parameters can be used as a proxy for secondary productivity.

Location: Northeast Pacific; 46–60° N and 125–165° W.

Time period: From 1998 to 2017 (ongoing).

Major taxa studied: Zooplankton, with a focus on large herbivores.

Methods: Approximately 280 summer zooplankton samples were analysed for carbon ($\delta^{13}C$) and nitrogen ($\delta^{15}N$) stable isotope (SI) ratios. Environmental conditions experienced by zooplankton organisms were extracted from satellite, in situ sensor and model databases. A generalized additive model approach was used to explain the spatial variability of $\delta^{13}C$ and $\delta^{15}N$ values and to predict isoscapes.

Results: Sea surface temperature (SST), sea level anomaly (SLA) and chlorophyll-*a* concentration emerged as the significant SI predictors. Modelled isoscapes reproduced patterns observed in $\delta^{13}C$ and $\delta^{15}N$ value distribution, such as a decrease from the coast to offshore. The contribution of eddies in enhancing local production in the open ocean was also well captured by the models. In the central part of the NE Pacific, higher SI values were correlated with higher large copepod biomass measured by the North Pacific Continuous Plankton Recorder (CPR) survey. However, in the area off the coast of British Columbia, high $\delta^{15}N$ variability appeared to be associated with episodic intrusions of coastal waters, demonstrating that caution is needed when interpreting sharp changes in SI ratios.

Main conclusions: Although the mechanisms driving SI ratio variability are complex, we demonstrate that a few parameters used as a proxy for some of these major mechanisms are able to produce successful isoscape models. This approach was proved useful to provide a qualitative estimate of secondary production, which can be particularly valuable in a region where few data are available.

KEYWORDS

food web, migration pathways, secondary productivity, stable isotopes, trophic baseline, zooplankton

1 | INTRODUCTION

Carbon ($\delta^{13}C$) and nitrogen ($\delta^{15}N$) stable isotope (SI) ratios are a powerful ecological tool with a wide range of applications. Carbon SI values are generally considered to fractionate relatively little along the food chain and are therefore useful to determine which primary producers support a food web (McCutchan, Lewis, Kendall, & McGrath, 2003). The strong correlation between sea water temperature, which controls aqueous CO_2 concentration, and $\delta^{13}C$ results in very similar distribution patterns in areas where $\delta^{13}C$ values experience minimal alteration through high primary production (low to moderate production). The greater enrichment of nitrogen isotopes from one trophic level to the next provides a means to estimate the trophic level of individuals, assuming knowledge of the enrichment factor between trophic levels (Post, 2002). Stable nitrogen isotopes can also be used to infer nitrogen sources (Montoya, Carpenter, & Capone, 2002), providing insights into the role of these sources and processes in food web structuring. The SI approach also provides the advantage of integrating information over a range of time determined by tissue turnover rates, thus smoothing small-scale variability.

Spatial distributions of SI values, also called "isoscapes", were first used in terrestrial environments, for example, to track animal origins (Hobson, 1999), and are now being used increasingly in marine environments (e.g., MacKenzie et al., 2011). Isoscapes defined at lower trophic levels provide information on the SI baseline, which is required to assess the relative trophic position of higher trophic levels (e.g., Jennings & Warr, 2003). They can also provide information on the relative productivity of different regions, because $\delta^{13}C$ and $\delta^{15}N$ values tend to reflect variable production rates of phytoplankton (Rolff, 2000). This is attributable to the preferential uptake by phytoplankton cells of molecules with lighter isotopes, resulting in relatively low ratios in non-limiting conditions and relatively high ratios in limiting environments (Montoya & McCarthy, 1995). Finally, isoscapes can be used to track the migration of animals within the area covered by the isoscape (Trueman, MacKenzie, & Glew, 2017; Trueman, MacKenzie, & Palmer, 2012).

The cost and logistical difficulties of working in the high seas results in few in situ data available for regions that cover most of the globe and where a large number of fish and other animals spend a part of, or their entire, life cycle. The high spatio-temporal resolution needed to resolve processes driving the variability in production of lower trophic levels is impossible to obtain by ship-based sampling over such vast areas, leading to uncertainties in determining foraging conditions or biological carbon export. In the last two decades, primary productivity in the open ocean has been described better using ocean colour from satellite data, revealing complex structures and spatio-temporal variability in even oligotrophic regions (Chavez et al., 1999). But although this type of data has provided new insights into the offshore areas of the world's oceans, there are associated limitations (e.g., cloud cover creating data gaps, only the surface layer is sampled) that prevent a full understanding of the mechanisms driving the spatial variability of production and estimates of the total primary production. Furthermore, it is still debatable how this primary production is correlated with secondary production, with factors such as assimilation efficiency linked to food quality determining the transfer of biomass through the food web (Dickman, Newell, González, & Vanni, 2008). For planktivorous fish or higher trophic levels, it is the biomass and quality of secondary producers that matters for efficient growth. A more accurate estimation of secondary production at broad scales is thus necessary in order to describe foraging conditions for higher trophic levels at sea and to improve calculations of biomass fluxes and estimates of the biological pump efficiency.

The offshore part of the Northeast (NE) Pacific epitomizes the data-poor high seas region and is poorly described in terms of secondary production. In the present study, based on samples from two major sampling programmes in the Northeast Pacific [Continuous Plankton Recorder (CPR) and Line P], we developed an approach based on generalized additive models (GAMs) to define isoscapes at the scale of the NE Pacific. Our objectives were as follows: (a) to model the variability in $\delta^{13}C$ and $\delta^{15}N$ values using parameters based on remotely measured environmental data; (b) to model isoscapes for 1998–2017; and (c) to determine whether isoscapes can be used as an index for secondary productivity.

2 | MATERIALS AND METHODS

2.1 | Sample collection

Zooplankton samples were collected through two historical and ongoing sampling programmes in the Northeast Pacific, the CPR and Line P (Figure 1; Table 1). Line P is a sampling programme that collects hydrological and biological data at discrete stations along a transect going from Vancouver to Ocean Station P (https://www.waterproperties.ca/linep/index.php). Six stations (P4, P8, P12, P16, P20 and P26 or OSP) were retained to be included in the study. The samples are collected from 200 m depth to the surface using a Bongo net. Samples for the time period 2009–2016 (except 2012) were included. The samples are routinely size fractionated and dried onboard (48 hr at 60 °C), and we kept only the size fraction 2–4 mm, which is usually dominated by large copepods (Goldblatt, Mackas, & Lewis, 1999).

Continuous Plankton Recorders were first deployed in the NE Pacific in 2000 along two transects. Detailed information about the sampling methodology and the historical background for CPR implementation in the NE Pacific are described by Batten et al. (2003). Briefly, the instrument is towed behind the ship, and plankton are sampled continuously from an approximate depth of 7 m, entering the sampler via a square aperture of 1.2 cm and being filtered by a silk gauze with a mesh size of 270 μm. A first batch of samples (n = 87) was run for SI analysis in the context of a pilot study. These samples covered the time period 2010–2013 and were analysed without performing any taxonomic separation (bulk zooplankton

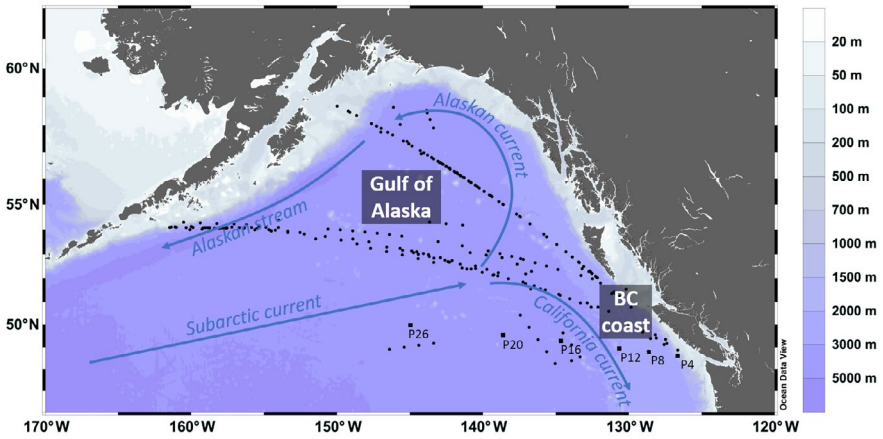

FIGURE 1 Map of the study area, indicating the location of zooplankton sampling from Continuous Plankton Recorder (CPR; black dots) and Line P programmes (black squares with station labels: P2, P8, P12, P16, P20 and P26)

TABLE 1 Summary of the sample sources, type and number

Programme	Time coverage	Sampling information	Sample type	Number of samples per year	Total number of samples
Line P	2009–2016 (except 2012)	Bongo net 200–0 m	Bulk, 2–4 mm size fraction	*n* = 7 for each year	*n* = 42
CPR, first batch	2010–2013	*c*. 7 m	Bulk	2010: *n* = 36; 2011: *n* = 22; 2012: *n* = 14; 2013: *n* = 15;	*n* = 87
CPR, second batch	2000–2009 and 2014–2017	*c*. 7 m	*Neocalanus* spp.	2000: *n* = 12; 2001: *n* = 16; 2002: *n* = 13; 2003: *n* = 12; 2004: *n* = 11; 2005: *n* = 15; 2006: *n* = 8; 2007: *n* = 11; 2008: *n* = 7; 2009: *n* = 7; 2014: *n* = 11; 2015: *n* = 11; 2016: *n* = 4; 2017: *n* = 11	*n* = 149
				Grand total	*n* = 278

analysis). However, all these samples were selected from a larger dataset and were described by the technician processing the samples as dominated by copepods. A second batch of 150 samples were retrieved for 2000–2017, for which large herbivorous zooplankton species (i.e., *Neocalanus* spp. at copepodite stage V) were removed from the samples.

We aimed to develop the isoscapes so that they could be used for studies of top predators (e.g., Pacific salmon) and therefore decided to focus on large copepods. *Neocalanus* spp. usually dominate the biomass in the Gulf of Alaska (GoA) in June when offspring reach sub-adult stages (Goldblatt et al., 1999). These herbivorous species build large reserves of lipids throughout the spring phytoplankton bloom and are important food sources for a number of top predators. Their annual production is driven by the size of the adult stock at the beginning of the reproductive season, but more importantly, by the environmental conditions that will promote (or not) the development of the new generation in spring to early summer (El-Sabaawi, Trudel, Mackas, Dower, & Mazumder, 2012; Sousa, Coyle, Barry, Weingartner, & Hopcroft, 2016).

When we use the term "secondary productivity" in this study, we refer to the biomass of the *Neocalanus* spp. in the NE Pacific. Three species were considered: *Neocalanus plumchrus*, *Neocalanus flemingeri* and *Neocalanus cristatus*. The potential bias that could result from using samples from different sources and with different species was investigated by comparing the mean of the SI values (see Supporting Information Appendix S1, Table S1.1). No differences were found between *N. plumchrus*/*N. flemingeri* and *N. cristatus* for both $\delta^{13}C$ and $\delta^{15}N$ values, in agreement with the literature (Chiba et al., 2012). The $\delta^{15}N$ values were significantly higher in bulk samples than in *Neocalanus*-sorted samples (6.69 vs. 6.19‰), but this appeared to be driven by higher $\delta^{15}N$ values for 2010 (7.00‰), which represented a large part of the bulk samples used in this analysis (36 out of 87 bulk samples).

2.2 | Sample selection

We aimed to model and predict isoscapes for the month of June as representative of summer conditions and the time period with the best interannual coverage. Accordingly, only zooplankton samples collected between 25 May and 15 July were considered. In addition, because the range of values and the processes behind SI variability can differ between shelf and offshore regions, we selected samples ≥ 50 km away from any shore. Therefore, when we mention coastal–offshore gradients, we refer to 50 km from the closest coast, and in most of the cases "coastal" is roughly located over the slope.

The majority of the samples included in development of the model were selected from the CPR catalogue using several criteria: a minimal presence of large copepods (about five individuals to ensure SI analysis viability); availability of chlorophyll-*a* (chl-a) estimates from satellite; and a sampling design thought to reduce the influence of spatial autocorrelation (no consecutive stations along a transect were used). The underlying rationale in sample selection was to build a dataset that would be as exhaustive as possible in terms of representing different environmental conditions and ecosystem states. To achieve that, the samples were picked randomly from within different sub-regions of the NE Pacific assumed to be different (i.e., Alaskan gyre, transitional domain and zone under eddy influence) and across hydrographic gradients (i.e., coastal–offshore gradient and Subarctic current).

2.3 | Stable isotope analysis

All samples were dried, homogenized and sent for SI analysis at UC Davis Stable Isotope Facility (https://stableisotopefacility.ucdavis.edu/13cand15n.html). The samples were analysed for ^{13}C and ^{15}N isotopes using a PDZ Europa ANCA-GSL elemental analyser interfaced to a PDZ Europa 20–20 isotope ratio mass spectrometer (Sercon Ltd, Crewe, UK). The system was calibrated using different NIST standard reference materials. Measurement precision was assessed by running replicates of these standards and resulted in an *SD* consistently < 0.1‰ both for $\delta^{13}C$ and $\delta^{15}N$. Isotopic ratios are expressed in the following standard notation:

$$\delta X\,(‰) = \left(\text{Rsample}/\text{Rstandard} - 1\right) \times 1000.$$

where X is ^{13}C or ^{15}N and Rsample is the $^{13}C/^{12}C$ or $^{15}N/^{14}N$, respectively. The $\delta^{13}C$ and $\delta^{15}N$ were determined in parts per thousand (‰) relative to external standards of Vienna Pee Dee Belemnite and atmospheric nitrogen, respectively. A lipid correction was applied to $\delta^{13}C$ values following the equation proposed by Smyntek, Teece, Schulz, and Thackeray (2007):

$$\delta^{13}C^{*} = \delta^{13}C + 6.3\left(\text{C:N} - 4.2\right)/\text{C:N}$$

where $\delta^{13}C^{*}$ is the $\delta^{13}C$ corrected for lipid effect and C:N is the ratio between the mass in carbon and nitrogen in the sample.

While Line P samples where dried directly on board, whereas CPR samples were preserved within formalin for a certain amount of time (usually 3 weeks). To correct for the effect of formalin and standardize both $\delta^{13}C$ and $\delta^{15}N$ values between programmes, we followed the recommendations of Bicknell et al. (2011) and applied appropriate correction factors depending on the way in which the samples were handled and the type of formalin used.

The large amount of anthropogenic carbon dioxide released into the atmosphere has led to a long-term decrease in both atmospheric and oceanic $\delta^{13}C$ values, known as the Suess effect (Gruber et al., 1999). The extent of this decrease is directly linked to the rate of change of CO_2 concentration and has therefore accelerated in recent decades. We applied a correction factor of −0.02‰/year, in agreement with recent studies (Espinasse, Hunt, Doson Coll, & Pakhomov, 2018; Williams, Risk, Stone, Sinclair, & Ghaleb, 2007). All data were standardized using 2000 as the year of reference.

2.4 | Data collection and preparation

Satellite data provide relevant spatio-temporal coverage of ocean conditions, and as such, were used to define a set of parameters that could be used to explain SI ratio variations. Data information and sources are summarized in Table 2. Data were extracted from the appropriate dataset to best fit the location and time of zooplankton sampling. A large set of parameters were defined and tested, including integration over different ranges of time. Tissue turnover in copepods is estimated to be *c*. 1–2 weeks (Graeve, Albers, & Kattner, 2005; Tiselius & Fransson, 2016), and therefore, variables should ideally be integrated over a similar time window. Good coverage for certain parameters allowed the extraction of exact matching data, whereas some other parameters required more flexibility to ensure data availability by widening the time and/or spatial windows (for integration in time and space of all the parameters, see Table 2).

Relationships between the modelled isotope values and secondary production were investigated using large copepod biomass from CPR samples. The offshore intrusion of smaller copepods transported from the coastal area into open ocean was assessed using the percentage of small-sized copepods in the total biomass (Mackas & Coyle, 2005). The cut-off size between small and large copepods was set at 2 mm total length. Small copepods comprise predominantly *Acartia longiremis*, *Pseudocalanus* spp., *Paracalanus* spp. and *Oithona* spp. Biomass was estimated based on an individual dry weight value per taxonomic entity multiplied by the taxon abundance. A total of 1,325 observations from 23 May to 5 July were gridded as a 1.5° × 1.5° resolution map, and then the biomass of large copepods and the percentage of small copepods were averaged for each year between 2000–2017. Both day and night samples were included, because we did not find any evidence of change in large copepod abundance between the two periods. Only grid cells containing data for ≥ 10 years were kept for the analysis.

2.5 | Model formation

All statistical models and analyses presented in this paper were made using the software environment R v.3.5.1 (R Core Team, 2018) together with the package ‘‘mgcv” (v.1.8–17; Wood, 2004, 2011) and model outputs were plotted using “mgcViz”. The first step consisted of data exploration and, more specifically, investigating the presence of outliers, collinearity between predictors and relationships between the response variable and the predictors (Zuur, Ieno, & Elphick, 2010). Predictors showing collinearity were not included at the same time during the model development procedure. Given that the functional forms between the response variable and the predictors are not known, and it was not obvious whether all relationships would follow a linear pattern, we opted

TABLE 2 Description of the parameters used in the generalized additive models

Parameter	Value range	Time window	Spatial window	Transformation	Notation	Data source
SST	4.8–13.3 °C	2 weeks	0.05° × 0.05°		SST	http://marine.copernicus.eu/; Id: SST_GLO_SST_L4_REP_OBSERVATIONS_010_011 (Merchant et al., 2014)
	4.8–13.1 °C	1 day (1 June)	0.05° × 0.05°		SST_150	
SST anomalies	−1.6 to 3.1 °C	Mid-June	0.05° × 0.05°			
Difference in SST	2.5–10.7 °C	SST sampling date minus SST mid-Feb	0.05° × 0.05°			
Sea level anomaly	−8 to 39 cm	1 week	0.25°		SLA	http://marine.copernicus.eu/; Id: SEALEVEL_GLO_PHY_L4_REP_OBSERVATIONS_008_047
chl-a	0.13–13.93 mg/m^3	2 weeks up to 4 weeks if data not available	4–9 km up to 25 km offshore[a] and 12 km close to the coast if data not available	Logged	chl-a	https://oceancolor.gsfc.nasa.gov/ SeaWiFs and MODIS-Aqua (2002-onwards)
	0.17–9.84 mg/m^3	From mid-Feb to sampling date	25 km offshore[a] and 12 km close to the coast	Logged	chl-a_4m	
Wind	6.3–9.8 m/s	Mid-Feb to sampling date	1.85°		winds	https://www.esrl.noaa.gov/psd/ NCEP_Reanalysis 2
Distance to the 200 m isobath	0–924 km		0.016°	Capped at 700 km	dist_200c	https://www.ngdc.noaa.gov/mgg/global/ETOPO1
Mixed layer depth	10.5–66.4 m	1 May to 31 July	1° up to 3° if data not available	Capped at 40 m	MLD	Argo floats (Hosoda, Ohira, Sato, & Suga, 2010) Thickness definition: $\Delta\sigma\theta$ = 0.03 kg/m^3 (de Boyer Montégut, Madec, Fischer, Lazar, & Iudicone, 2004)

Note: Data were extracted and processed to be as close as possible to the sampling date and location.
Abbreviations: chl-a = chlorophyll-*a*; MLD = mixed layer depth; SST = sea surface temperature.
[a]Delimitation between coastal and offshore area is 100 km from the coastline.

for a GAM. Nonparametric models provide more flexibility to fit the data by using smoothers while still leaving the possibility of using a generalized linear model if linear relationships emerge later. The smoothing parameters are estimated by penalized likelihood maximization, in order to find a balance between wiggliness of the smoothers (overfitting) and deviance of the model (Wood, 2011). The model also estimates the basic dimension of the smoother *k* to minimize the Akaike information criterion (AIC; Akaike, 1974), which is a non-dimensional estimator of the explanatory power of the model compared with its complexity. The predictors were selected using a backward-elimination procedure, in which the least significant predictor was removed until all remaining effects were significant. Interaction terms have also been considered. The selection between the different models was made as a trade-off between significantly reducing the AIC and obtaining relationships between predictors and the response variable that made sense from an ecological point of view. All the models presented in the paper were validated by checking the homogeneity of variance and the normal distribution of residuals and by investigating any pattern in the plot of residuals against predictors (Zuur, 2012). Also, residuals were investigated considering the year, day of the year, latitude and longitude to test whether these parameters were influential.

2.6 | Production of isoscapes

Once the model was developed and validated, we aimed to predict SI values over the whole NE Pacific. All datasets were adapted to fit in a 0.25° × 0.25° spatial grid. Spatial integration windows were set wider for chl-a than during the first step (Table 2), to ensure good coverage. Mixed layer depth (MLD) data were interpolated using the scatteredInterpolant function in Matlab 2018a. Nitrogen and carbon SI ratios were then predicted using the function predict.gam included in the "mgcv" package. The isoscapes were produced for the period 1998–2017, considering mid-June as the reference time and covering the region spanning from 46 to 60° N and from −165 to −125° W, in agreement with sampling data coverage.

3 | RESULTS

3.1 | Model performance and validation

Zooplankton samples have δ^{15}N values spanning from 1.4 to 12.5‰ and δ^{13}C values from −27.7 to −18.9‰. The selective process run on all the parameters defined δ^{13}C and δ^{15}N models as follows (for the meaning of abbreviations, see Table 2; *s* stands for smooth class, thin plate regression splines in this case):

$$\text{Model 1:}\delta^{13}\text{C} \sim s(\text{chla}) + s(\text{SLA}) + \text{SST\_150} + s(\text{dist\_200c})$$

$$\text{Model 2:}\delta^{15}\text{N} \sim s(\text{chla\_4m}) + s(\text{SLA}) + s(\text{SST}) + s(\text{MLD})$$

however, the limited spatial coverage for MLD led us to develop a second N model that did not include this predictor:

$$\text{Model 3:}\delta^{15}\text{N} \sim s(\text{chla\_4m}) + s(\text{SLA}) + s(\text{SST})$$

The GAM results are summarized in Table 3 and Figures 2 and 3. The δ^{15}N model that included MLD performed better in terms of variance explained, but the spatially heterogeneous availability of MLD data (see Supporting Information Appendix S1, Figure S1.1) did not allow the production of isoscapes for the entire study area, and therefore, the model with MLD will not be presented further here.

The significance of the different smoothers was estimated by running the model with unpenalized smoothing using the basic dimension defined by the penalization procedure. Sea surface temperature

TABLE 3 Generalized additive model results for the two δ^{15}N models, with and without mixed layer depth, and for the δ^{13}C model

	Model 1: C model	Model 2: N model	Model 3: N model with MLD
Intercept	−23.29***	6.59***	7.45***
Predictors			
SST	NA	3.00***	3.20***
SLA	5.29***	4.45***	1.70**
chl-a	5.09*	NA	NA
chl-a_4m	NA	2.29***	1***
SST_150	1**	NA	NA
dist_200c	1.98***	NA	NA
MLD	NA	NA	8.07***
No. of observations	262	271	241
Total *df*	14.36	8.74	14.97
Deviance explained (%)	43.3	50.7	59.5

Abbreviations: MLD = mixed layer depth; SLA = sea level anomaly; SST = sea surface temperature. Intercept values are shown, in addition to the degrees of freedom for the predictors. The total degrees of freedom used by each model is also mentioned.
*p < .05; **p < .01; ***p < .001.

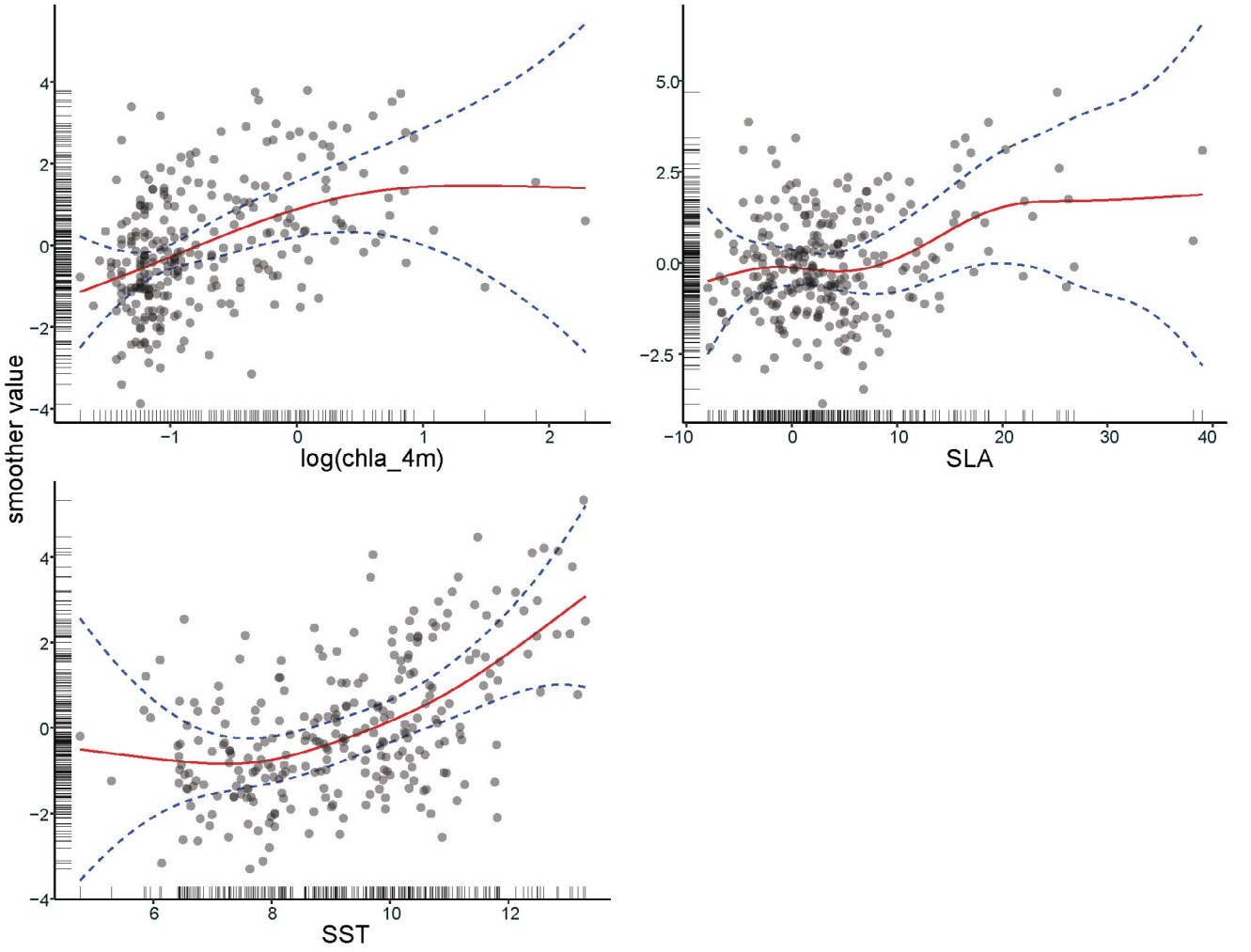

FIGURE 2 Smoother values associated with chlorophyll-*a* (chl-a) concentrations averaged over spring, sea level anomaly (SLA) in mid-June and sea surface temperature (SST) in mid-June, used to model $\delta^{15}N$ values with the generalized additive model approach. Residuals date (grey dots) and 95% confidence interval (blue dashed lines) are displayed

(SST) had a strong predictive power in all models. Considering the $\delta^{13}C$ model (Model 1), the SST value at 1 June was more significant than the SST at the time of sample collection. One of the difficulties with the $\delta^{13}C$ model was to deal with the cold but productive coastal water adjacent to the Aleutian Islands, which were characterized by high $\delta^{13}C$ values. Adding as a parameter the distance to the 200 m isobath partly solved this problem (most significant parameter for the $\delta^{13}C$ model). The chl-a concentrations integrated over 4 months and sea level anomaly (SLA) were the second most significant predictors for $\delta^{15}N$ and $\delta^{13}C$ models, respectively. A subset of the isoscapes is shown for the most recent 6 years (2012–2017), covering large changes in environmental conditions, including the presence of a warm anomaly observed in 2014 (Bond, Cronin, Freeland, & Mantua, 2015; Whitney, 2015; Figures 4 and 5; chl-a, SST and SLA are shown in Supporting Information Appendix S1, Figures S1.2, S1.3 and S1.4). The distributions of the residuals over the years showed no extreme values for the $\delta^{13}C$ and $\delta^{15}N$ models (Supporting Information Appendix S1, Figures S1.5 and S1.6). Spatial distribution of the residuals did not display any particular pattern either, with residuals seeming to be distributed randomly over the study area (Supporting Information Appendix S1, Figure S1.7).

Uncertainties of the model outputs were investigated using *SE* associated with predicted SI values (Figures 6 and 7). Both models displayed the highest level of uncertainty in places corresponding to eddy locations. Elsewhere in the GoA, the $\delta^{15}N$ model showed lower *SE* (mainly < 0.2) than the $\delta^{13}C$ model, except in places with SST outside the normal range (< 4 and > 13.5 °C). In general, the models showed a good agreement with observational data by reproducing general patterns adequately (Supporting Information Appendix S1, Figures S1.8 and S1.9).

Similarities between the $\delta^{15}N$ and $\delta^{13}C$ isoscapes were observed for most of the years, especially the eddy signatures and the coastal–offshore gradients. The amplitude of the gradient from coast to offshore was, however, higher for $\delta^{15}N$ values than for $\delta^{13}C$ values. Interannual variability was assessed for $\delta^{13}C$ and $\delta^{15}N$ values using the *SD* in each grid cell (Figure 8). The variability was moderate in the North part of the G0A and in general along the coast for both $\delta^{13}C$ and $\delta^{15}N$ values. Relatively high variability was observed off the British Columbia (BC) coast for $\delta^{15}N$ values.

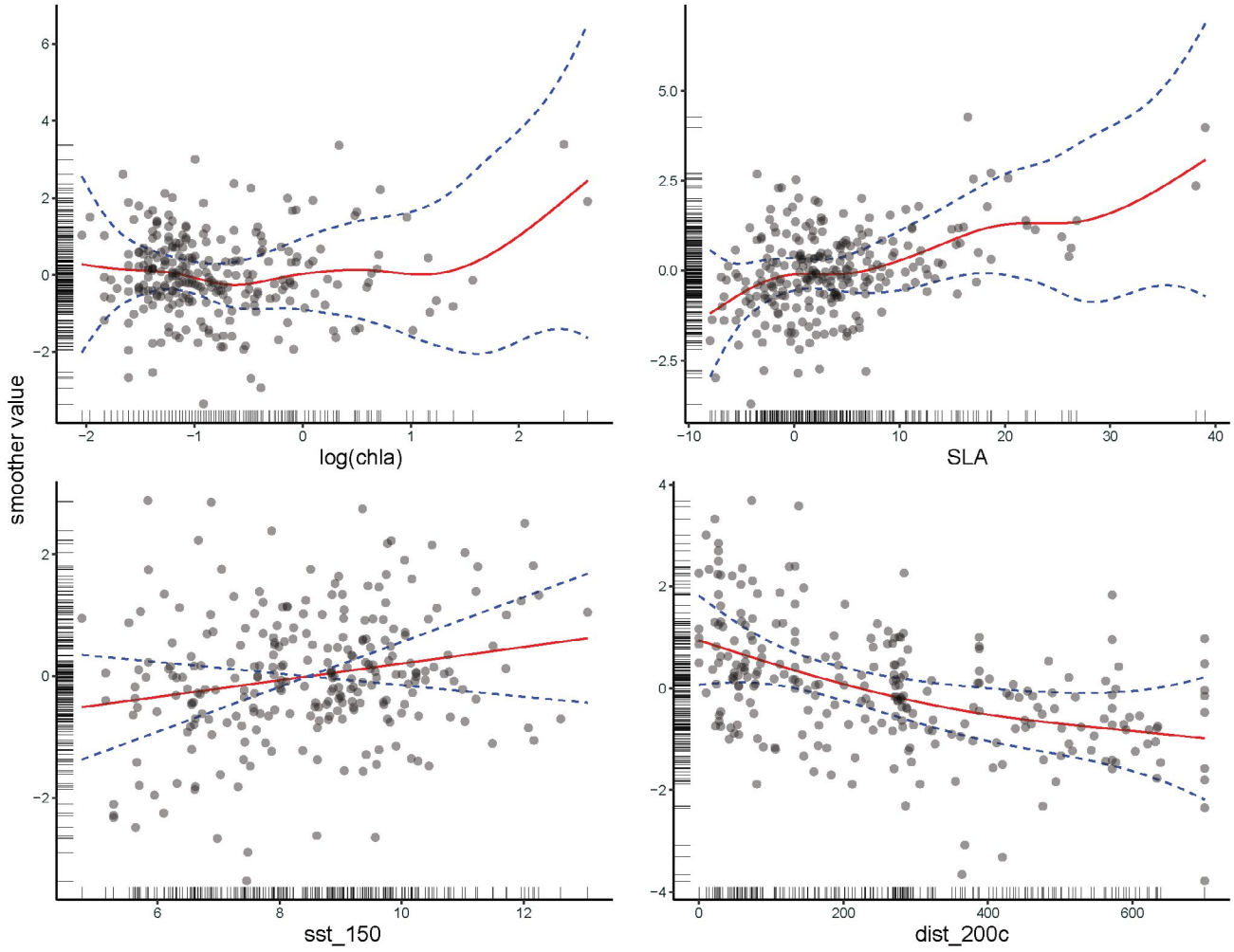

FIGURE 3 Smoother values associated with chlorophyll-*a* (chl-a) concentrations, sea level anomaly (SLA) in mid-June, sea surface temperature (SST) in mid-June and distance to the 200 m isobaths, used to model $\delta^{13}C$ values with the generalized additive model approach. Residuals date (grey dots) and 95% confidence interval (blue dashed lines) are displayed

3.2 | Stable isotope versus zooplankton biomasses

Relationships between modelled SI values and parameters characterizing the zooplankton community were assessed using Pearson correlation (Figure 9). The sign and significance of the correlation coefficient defined three main areas constrained along CPR transects, namely the North part of the Gulf of Alaska (NGoA), the South part of the Gulf of Alaska (SGoA) and the area off the BC coast. Both the NGoA and the SGoA showed an increase in large copepod biomass with higher $\delta^{15}N$ and $\delta^{13}C$ values. In contrast, off the BC coast lower biomasses were associated with higher SI values. Considering the relative contribution of small-sized copepods to total biomass, the BC coast showed a positive correlation and SGoA a negative correlation, while the sign of the correlation was undetermined in NGoA considering $\delta^{13}C$ values. Small copepod biomass was, in general, positively correlated with $\delta^{15}N$ values, except in the SGoA. Information was summarized by pooling the data in grid cells that showed similar correlation sign in the GoA (North and South pooled together) and along the BC coast sub-regions. Large copepod biomass was generally higher in the GoA than off BC, and the interannual variability was lower in the GoA than off the BC coast for 2000–2017 (Figure 10). The $\delta^{13}C$ and $\delta^{15}N$ values presented similar general trends between areas, although with higher values along the BC coast than in the GoA. However, large copepod biomasses showed different trends, resulting in the opposing dynamics observed in Figure 9.

4 | DISCUSSION

The aim of the present study was to test the application of isoscapes modelled from satellite data to the description of secondary production in the ocean. Significant correlations between modelled SI values and large copepod biomass demonstrated the relationship between these parameters. However, it is important to understand the underlying physical and biogeochemical processes in this relationship in establishing the model limits and the potential for exporting the method to other regions, and we discuss this in detail below.

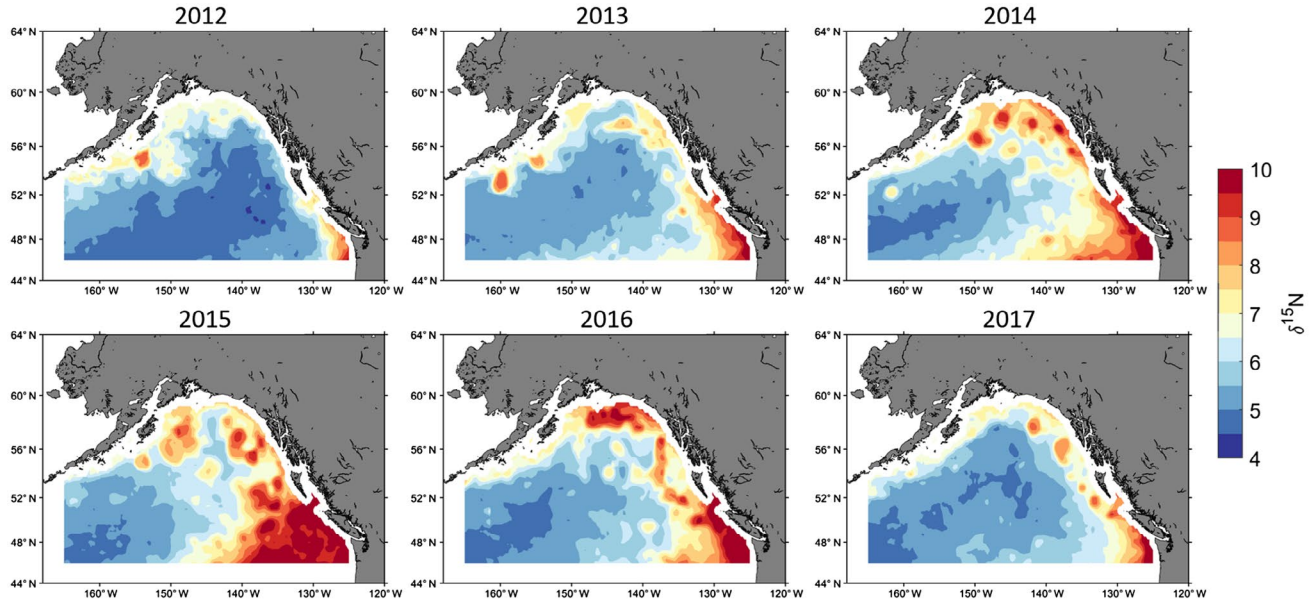

FIGURE 4 Isoscapes of $\delta^{15}N$ values modelled using a generalized additive model approach for 2012–2017

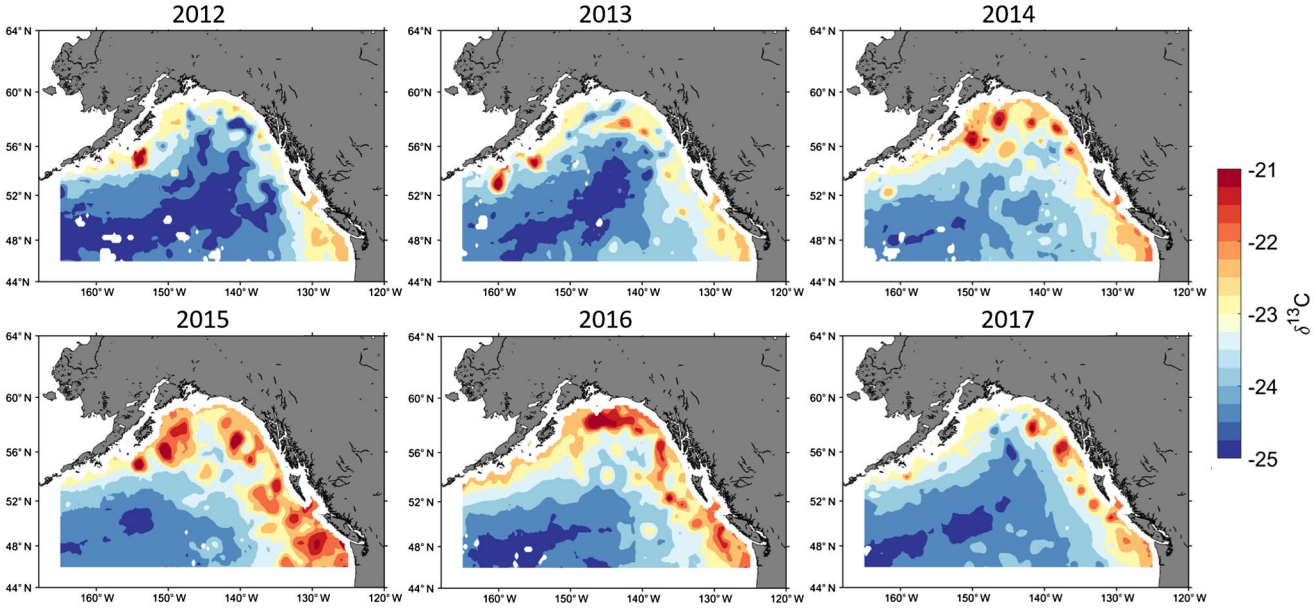

FIGURE 5 Isoscapes of $\delta^{13}C$ values modelled using a generalized additive model approach for 2012–2017

4.1 | Environmental drivers and biogeochemical processes controlling SI

In the present study, SST, chl-a and SLA were the most significant parameters for quantifying and predicting $\delta^{13}C$ and $\delta^{15}N$ values in our models. The modelled isoscapes show some consistent patterns through the years, such as a coastal–offshore gradient, eddy locations characterized by higher $\delta^{13}C$ and $\delta^{15}N$ values, and higher values in warmer years (as can be seen in Figures 4 and 5 during the 2014 marine heatwave). A decrease of $\delta^{13}C$ and $\delta^{15}N$ values from the shelf to offshore is usually observed in the marine environment as a result of higher productivity close to the coast, enhanced by greater nutrient availability owing to terrestrial input and shallower water that promotes water mixing down to the sea bottom and resuspension of nutrients (El-Sabaawi et al., 2012; Kline, 2009). Shallower waters also warm faster at the beginning of the summer season, and SST together with chl-a are usually good proxies to represent coastal influence and to reproduce the coastal–offshore gradient.

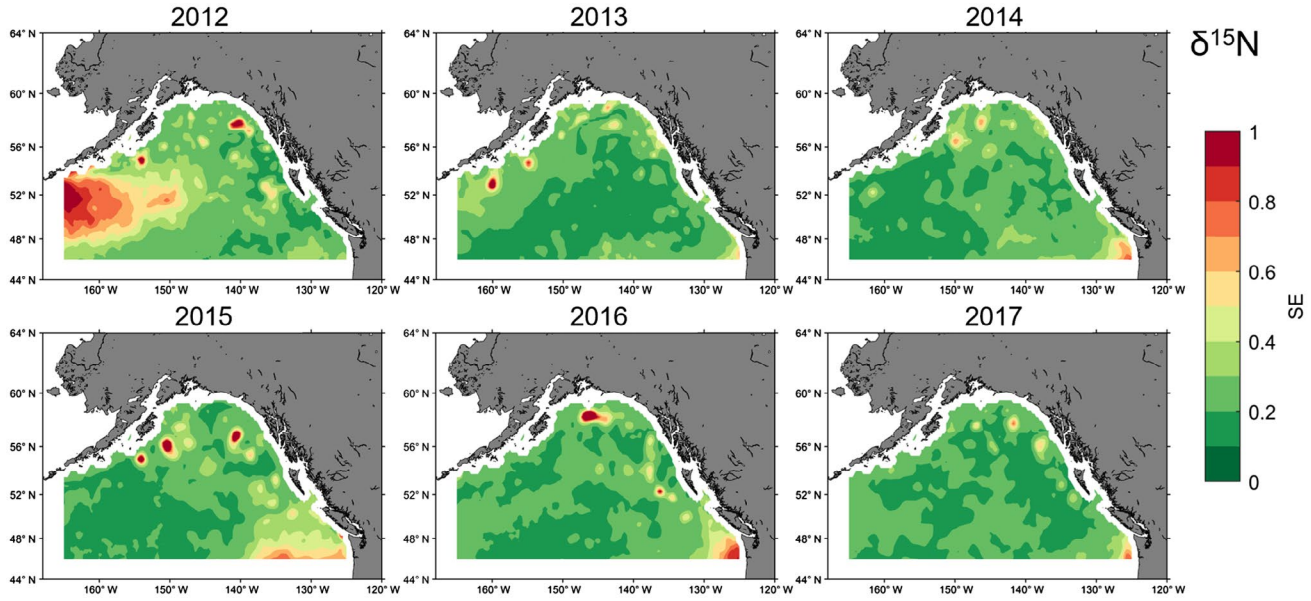

FIGURE 6 Standard error associated with $\delta^{15}N$ values modelled using a generalized additive model approach for 2012–2017

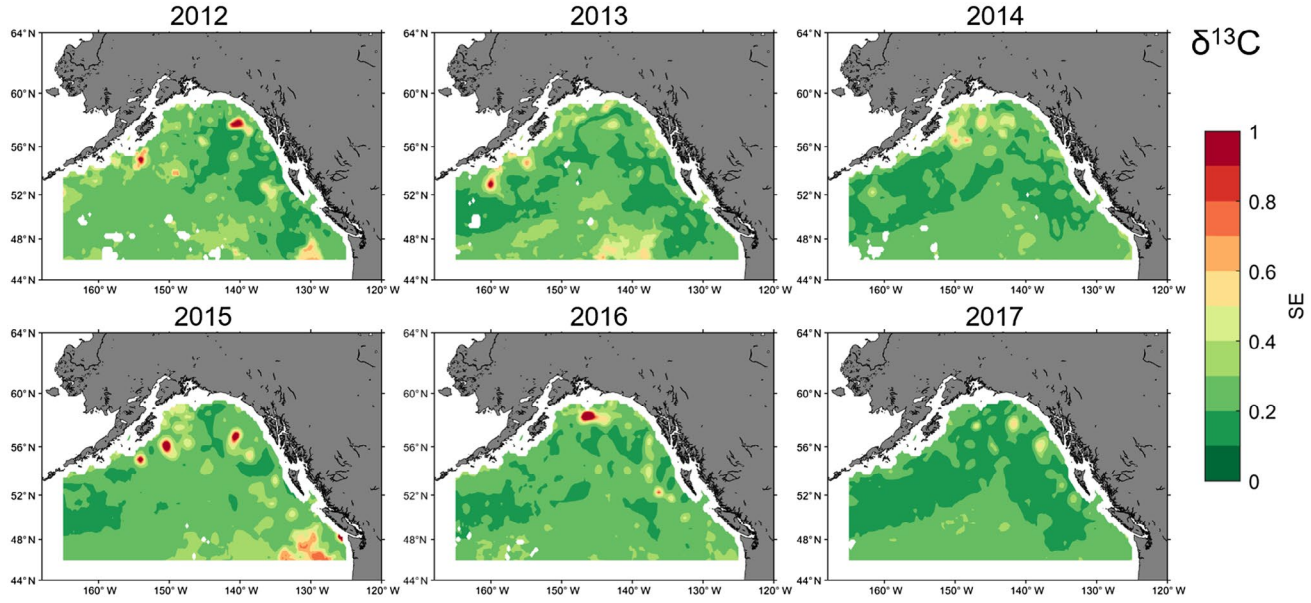

FIGURE 7 Standard error associated with $\delta^{13}C$ values modelled using a generalized additive model approach for 2012–2017

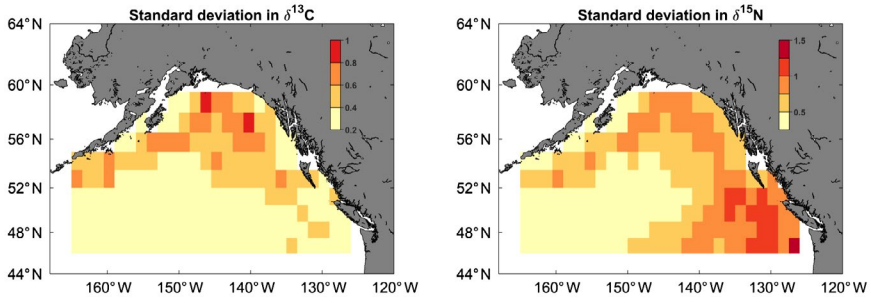

FIGURE 8 Interannual variability of modelled $\delta^{15}N$ and $\delta^{13}C$ values for 1998–2017

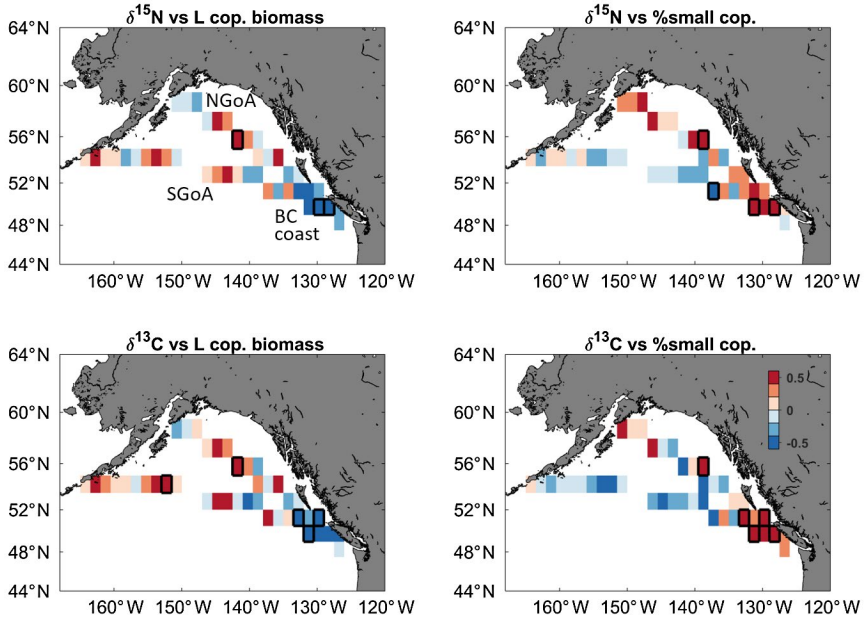

FIGURE 9 Pearson correlation coefficient between large copepod biomasses and percentage of small-sized copepod biomass (< 2 mm) from Continuous Plankton Recorder (CPR) samples and the modelled $\delta^{15}N$ and $\delta^{13}C$ values for 2000–2017. Significant correlations ($p < .05$) are indicated by a black frame. Three sub-regions (NGoA and SGoA = the North part and South part of the Gulf of Alaska, respectively; BC coast = the region off the British Columbia coast) were defined for further analysis

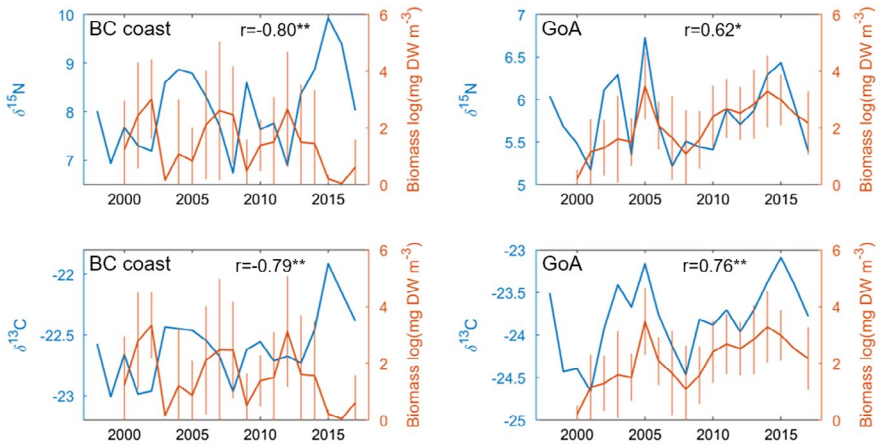

FIGURE 10 Time series of logged large copepod biomass from the Continuous Plankton Recorder (CPR) programme (red lines), modelled $\delta^{15}N$ values (top, blue lines) and modelled $\delta^{13}C$ values (bottom, blue lines) in the area off the British Columbia coast (left) and the pooled north and south Gulf of Alaska (right) for 1998–2017. Standard deviation is indicated by vertical bars for the copepod abundance. The correlation coefficient (*r*) for each relationship is shown. $^{*}p < .01$; $^{**}p < .001$

Given that we focused on large, herbivorous copepods, we assumed that the offset between phytoplankton SI values and the modelled SI was consistent. The main factors that would then explain the variation in SI were the uptake processes at the base of the food web and the composition of the phytoplankton community. The different biogeochemical processes behind variation in the SI ratios at the base of the food web have been examined extensively in the last two decades (Bowen, 2010; McMahon, Hamady, & Thorrold, 2013; Montoya, 2008). They revolve around nutrient uptake dynamics and are largely driven by nutrient/CO_2 availability. Values for $\delta^{13}C$ were recently modelled at the scale of the globe by Magozzi, Yool, Vander Zanden, Wunder, and Trueman (2017). These authors demonstrated that sea temperature, through control of aqueous CO_2 concentration, was the main factor controlling $\delta^{13}C$, even though a range of processes can influence the photosynthetic carbon isotope fractionation (e.g., phytoplankton composition, growth rates, cell permeability characteristics and photosynthetic pathways; Burkhardt, Riebesell, & Zondervan, 1999). The presence of diatoms, for example, will result in a phytoplankton pool having higher $\delta^{13}C$ and $\delta^{15}N$ values. Peña, Nemcek, and Robert (2018) found that the 2014 marine heatwave resulted in an increase in diatom abundance at the offshore part of Line P (central part of the NE Pacific), and this signal was well captured in the modelled isoscapes, with relatively high $\delta^{13}C$ and $\delta^{15}N$ values offshore (Figures 4 and 5). Among the processes described by Somes et al. (2010) as affecting phytoplankton $\delta^{15}N$ values, NO_3^- uptake is arguably the more likely to dominate in the NE Pacific. By drawing down nitrate concentrations, high phytoplankton biomasses result in an increase in $\delta^{15}N$ values. Therefore, nitrate-limited areas over the continental shelf show higher $\delta^{15}N$ values that will spread offshore to varying degrees depending on physical processes. Ideally, chl-a concentration should have been averaged over 1- to 2-week intervals in our study, but patchy data availability owing to cloud coverage necessitated a balance between the optimal integration time window and data availability (both for model building and for prediction). The 2–4 week integration used reduced potential bias of patchy data integrated over short time windows (e.g., high cloud coverage resulting in either missing a bloom or having only bloom data).

An important mechanism of shelf–offshelf exchanges in the NE Pacific is the offshore transport of coastal water by eddies (Henson

& Thomas, 2008). Sea level anomaly is a useful parameter to track these eddies. In the Northern Hemisphere, anticyclonic eddies tend to accumulate water in their centre under the effect of the Coriolis force, resulting in higher sea surface height and, thus, positive sea level anomalies. The eddies in the GoA originate near the coast and therefore have the potential to introduce iron to the otherwise iron-depleted offshore water, enhancing primary production, and will then be colonized by offshore species (Mackas, Tsurumi, Galbraith, & Yelland, 2005). The increase in phytoplankton draws down NO_3^- concentrations, resulting in a proportional increase in $\delta^{15}N$ values, although these values will not reach those encountered in NO_3^--limited environments, such as coastal areas. To the best of our knowledge, this is the first time that a direct link between high isotope values and high SLA has been demonstrated. Mixed layer depth can relate to other key processes, such as stratification strength, that will control iron input from deep waters, and it was therefore not surprising that the $\delta^{15}N$ model (Model 3) that include MLD as a parameter worked better. With the increase in Argo float deployment, it seems likely that MLD will be a parameter commonly used in the development of future isoscapes.

A few additional nitrogen cycling-related uptake processes may influence $\delta^{15}N$ values and might be captured to different degrees by the models. Denitrification, for example, leads to an increase in $\delta^{15}N$ values and usually occurs in anoxic environments (Williams, Wakeham, McKinney, & Wishner, 2014). However, although there is a trend towards a decrease in oxygen concentration in the NE Pacific (Crawford & Peña, 2016), current pelagic oxygen levels are still above values found in oxygen minimum zones, and therefore, denitrification is not expected to be a factor in the epipelagic zone. Another process is biological nitrogen fixation, which has recently been shown to be a process occurring not only in tropical and subtropical environments (Horii, Takahashi, Shiozaki, Hashihama, & Furuya, 2018; Needoba, Foster, Sakamoto, Zehr, & Johnson, 2007), but that does seem to be restricted to environments with low nitrate concentrations. Nevertheless, lower than equilibrium N:P ratios caused by a phytoplankton bloom after an input of iron to the system could result in the development of diazotrophic cyanobacteria that will use the remaining phosphate pool. The lower $\delta^{15}N$ values associated with nitrogen fixation have been demonstrated to transfer to higher trophic levels, resulting in zooplankton grazer $\delta^{15}N$ values of < 2‰ (Montoya et al., 2002). Low $\delta^{15}N$ values may also occur owing to high nitrogen recycling and ammonium uptake (Pennock, Velinsky, Ludlam, Sharp, & Fogel, 1996), or phytoplankton size differences in nitrogen uptake (Karsh, Trull, Lourey, & Sigman, 2003). Only two (out of 278) of our samples had $\delta^{15}N$ values < 2‰ in our study, and therefore, we expect that neither of the aforementioned processes was a factor, but they might become major factors in changing ocean conditions in the future.

4.2 | Isoscape accuracy and limitations

The sample selection strategy was aimed purposefully to reduce unwanted variance as much as possible. The construction of isoscapes using field sampling should ideally use data collected as a temporal snapshot to avoid the effect of seasonal variability overwhelming the spatial variability (Kurle & McWhorter, 2017). The same limitation occurs with modelled isoscapes. In the present study, the data used to build our model were collected within a time window of 50 days. The boundaries of the time window were defined with the purpose of limiting the impact of potential seasonal variability by starting in late May, at the end of the productive season. By this time, the spring phytoplankton bloom has finished, and large herbivorous copepods have mainly reached copepodite stage V (Batten & Mackas, 2009).

The map of residuals and the inspection of their distribution along latitude and longitude did not reveal spatial patterns indicative of spatial autocorrelation (Supporting Information Appendix S1, Figure S1.7). In addition, semivariograms produced to explore changes in variance as a function of distance between sampling locations did not reveal any pattern suggestive of autocorrelation (Fortin & Dale, 2005). Mapping of the *SE* associated with the predicted SI values was useful to define the conditions in which the model performed the best and the model limitations (Figures 6 and 7). The models resolved the SI variability in the NE Pacific well, with the exception of two situations. First, the few samples collected in the vicinity of the eddies did not provide enough information to the models for production of accurate SI estimations associated with high SLA values. We showed that the SI values were higher close to the eddies, but we could not define their extent precisely. Second, prediction of $\delta^{15}N$ values with SST outside the range defined by the conditions sampled (4.8–13.3 °C) resulted in high uncertainty. This was clearly apparent in 2012, when unusually cold water spread into the western part of the study area, and in 2014–2015, when unusually warm conditions associated with the marine heatwave occurred in the southeast part of the NE Pacific.

Given that coastal environments are characterized by a different SI dynamic owing to shallower water and terrestrial influence, the 50 km strip along the coastline was excluded from the model for both development and prediction. This removed the strong $\delta^{13}C$ gradient and, to a lesser extent, $\delta^{15}N$ gradient, that occurs from the coastline to the continental slope, and allowed better contrast in the definition of spatial variability occurring in the open ocean. In general, the models adequately reproduced the coastal–offshore gradient seen in observational data, probably for the reasons explained above, which was anyways expected for the $\delta^{13}C$ model because the distance to the coast is one of the predictors, but not granted for the $\delta^{15}N$ model. Comparison with data collected along Line P showed greater variability in observational data than can be explained by variations in community composition (bulk samples; see Section 2) and/or processes that are unlikely to be captured by the model. Transport of organisms may also result in a slight spatial mismatch between observational and modelled data. The tissue turnover in copepods is assumed to be *c.* 1–2 weeks, but it is likely to be linked strongly with feeding activity, and by mid-June large herbivores usually slow down their activity depending on the environmental conditions (Dagg, Liu, & Thomas, 2006). This results in copepods that potentially retain a

constant SI value over a longer period of time and can explain the spatial mismatch in areas where stable circulation patterns will transport organisms.

4.3 | Ocean productivity index

Correlation between modelled SI values and large copepod biomass revealed two sub-regions, the GoA and off the coast of BC, characterized by positive and negative signs, respectively. Positive correlation in the GoA can be interpreted as a result of more productive waters leading to higher recruitment in copepods that grow throughout the spring. Higher productivity and/or development of larger phytoplankton is characterized by higher SI values. This supports the idea that both $\delta^{13}C$ and $\delta^{15}N$ values can be used in the GoA as an index of productivity for large copepods. Moreover, the negative correlation found along the BC coast is less intuitive. It was previously reported (El-Sabaawi et al., 2012) and was suggested to be attributable either to transport of organisms from other areas or to a change in nutrient availability. Based on bulk sample measurements, the authors concluded that variation in nutrient availability is likely to be the dominant factor controlling zooplankton SI along the BC coast. However, the direct negative correlation that we found between SI values and large herbivorous copepod abundance seems more likely to be explained by the presence of individuals that had fed within the last weeks in productive coastal shelf waters, characterized by higher SI values (Kline, 2009), before being transported offshore. This area is not the core distribution for *Neocalanus* species, and we suggest that in some circumstances there is a shift in community through the transport of shelf community copepods to the open ocean. This would explain both the low abundance of *Neocalanus* spp. and their higher SI values. In this specific case, the variation in SI is not linked with variation in secondary productivity (of large copepods) but is attributable to alternation between two different communities: the coastal community dominated by small copepods and low *Neocalanus* spp. abundance, with high SI values, and the offshore community dominated by large copepods, with lower SI values. Many studies have reported intrusion of warmer water or shelf copepods in this area owing to different physical processes, such as upwelling (Mackas & Coyle, 2005), eddies (Mackas & Galbraith, 2002) or a change in the normal circulation pattern (North Pacific current bifurcation index; Batten & Freeland, 2007). This was supported by the high interannual variability observed in the modelled $\delta^{15}N$ values along the BC coast (Figure 8).

4.4 | Other uses of isoscapes

In addition to providing information about ocean productivity and how environmental conditions can influence ecosystem processes (food quality, transfer efficiency, etc.), the isoscapes produced in the present study provide useful isotope baselines for trophic studies on higher trophic levels. They facilitate interpretation of historical time series of fish SI values, allowing the separation of shifts in baseline SI values from changes in food chain length (e.g., Pethybridge et al., 2018).

Another potential use is to compare SI values of fish or other migrating organisms with modelled SI values. In this case, it is necessary to estimate the trophic enrichment expected between the predator and prey. This can be straightforward if large herbivorous zooplankton, which have a known trophic position, are the main prey for the organisms studied. If not, then the relative difference in trophic position between the predator of interest and large herbivorous zooplankton has to be estimated. The spatial comparison of predator and prey SI values will then allow the definition of potential feeding areas for the predators. The location of fish at sea will be averaged over the tissue turnover time, which differs greatly depending on the type of tissue. Ideally, using a tissue/element with reasonably short turnover rates in an environment with a well-defined and stable SI gradient can give straightforward results (Jaeger, Lecomte, Weimerskirch, Richard, & Cherel, 2010), but new methods have also been developed for improving accuracy and precision in estimated feeding location with success (Trueman et al., 2017; Vander Zanden et al., 2015; Wunder, 2012).

4.5 | Exporting the method

Changes in the primary processes controlling SI values occur through major climate shifts, such as the 1977 NE Pacific regimen shift (Hare & Mantua, 2000), and raise questions about the robustness of the model over long time-scales. Stable isotope values seem to be reasonably stable over long time periods (Espinasse et al., 2018; Finney, Gregory-Eaves, Sweetman, Douglas, & Smol, 2000), and the main geographical gradients also appear to be consistent (MacKenzie, Longmore, Preece, Lucas, & Trueman, 2014). Our dataset covering 1998–2017 includes the 2014 marine heatwave event that increased the range of environmental conditions processed by the models. This suggests that the model might indeed be robust over time and allow the extension of the modelled period. Therefore, the production of new isoscapes in the future, when new data are available, is possible. However, extension to the past is limited by satellite data availability and would be dependent on reconstructed datasets.

It has been questioned whether models can be used to create isoscapes outside of the area for which they were designed (Barnes, Jennings, & Barry, 2009), because the processes of uptake and transfer along the trophic chain might differ between areas, reflecting differences in micronutrient/macronutrient limitation, intensity and duration of the productive season, and the impact of physical processes. The subarctic North Pacific together with the Southern Ocean and the Eastern Equatorial Pacific are all high-nutrient, low-chlorophyll regions (Lalli & Parsons, 1997). But, because sea temperatures in these regions span different ranges, the models developed in the present study should not be applied to these areas without including new SI data in the model development. Furthermore, the role played by the eddies in the subarctic North Pacific does not apply everywhere, and the structure of the model, such as the significant parameters, could differ in other regions.

Extending the isoscapes presented here westwards could be an option if SI data covering the Northwest Pacific were available either to validate the model in this area and/or to include them in the model development.

However, because the parameters describing SI variation in the present study, with the exception of the SLA, have been reported in many studies, we think that our general approach could be exported to other regions, provided that zooplankton samples were available with sufficient spatio-temporal coverage to allow development of similar models. Furthermore, development of new methods allows for the production of isoscapes based on different data sources while keeping model uncertainties low (St. John Glew, Graham, McGill, & Trueman, 2019). A good knowledge of the system is required to understand SI value variations, for example, the situation where higher SI values are not necessarily associated with higher secondary productivity. In particular, high SI variability can help to identify areas under coastal influence and where SI values will be affected sporadically by the higher SI baseline occurring on the shelf. This is particularly true for $\delta^{15}N$, for which the coastal signature can be observed far off the shelf. Taking that into account, we have demonstrated that, based on a few easily accessible parameters, it is possible to provide an estimate of relative zooplankton production through SI values.

ACKNOWLEDGMENTS

This project was supported by the Monell and Vetlesen Foundations. Pacific CPR sample and data collection is supported by a consortium for the North Pacific CPR survey coordinated by the North Pacific Marine Science Organisation (PICES) and comprising the North Pacific Research Board (NPRB), Exxon Valdez Oil Spill Trustee Council (EVOS TC), Canadian Department of Fisheries and Oceans (DFO) and the Marine Biological Association, UK. We thank DFO (M. Galbraith and I. Perry) for providing the zooplankton samples from Line P for analysis in this project.

DATA AVAILABILITY STATEMENT

Stable isotope data along with parameter values used to develop the models are provided in the Supporting Information (Appendices S2 and S3). The isoscapes produced in the present study are available on Dryad Digital Repository (https://doi.org/10.5061/dryad.d2547d7z6), in addition to updated versions as satellite data become available.

ORCID


Boris Espinasse https://orcid.org/0000-0002-7490-5588

REFERENCES

Akaike, H. (1974). A new look at the statistical model identification. *IEEE Transactions on Automatic Control*, *19*(6), 716–723. https://doi.org/10.1109/TAC.1974.1100705

Barnes, C., Jennings, S., & Barry, J. T. (2009). Environmental correlates of large-scale spatial variation in the $\delta^{13}C$ of marine animals. *Estuarine, Coastal and Shelf Science*, *81*(3), 368–374. https://doi.org/10.1016/j.ecss.2008.11.011

Batten, S. D., Clark, R., Flinkman, J., Hays, G., John, E., John, A., … Walne, A. (2003). CPR sampling: The technical background, materials and methods, consistency and comparability. *Progress in Oceanography*, *58*(2-4), 193–215. https://doi.org/10.1016/j.pocean.2003.08.004

Batten, S. D., & Freeland, H. J. (2007). Plankton populations at the bifurcation of the North Pacific Current. *Fisheries Oceanography*, *16*(6), 536–546. https://doi.org/10.1111/j.1365-2419.2007.00448.x

Batten, S. D., & Mackas, D. L. (2009). Shortened duration of the annual *Neocalanus plumchrus* biomass peak in the Northeast Pacific. *Marine Ecology Progress Series*, *393*, 189–198. https://doi.org/10.3354/meps08044

Bicknell, A. W. J., Campbell, M., Knight, M. E., Bilton, D. T., Newton, J., & Votier, S. C. (2011). Effects of formalin preservation on stable carbon and nitrogen isotope signatures in Calanoid copepods: Implications for the use of Continuous Plankton Recorder Survey samples in stable isotope analyses. *Rapid Communications in Mass Spectrometry*, *25*(13), 1794–1800. https://doi.org/10.1002/rcm.5049

Bond, N. A., Cronin, M. F., Freeland, H., & Mantua, N. (2015). Causes and impacts of the 2014 warm anomaly in the NE Pacific. *Geophysical Research Letters*, *42*(9), 3414–3420. https://doi.org/10.1002/2015GL063306

Bowen, G. J. (2010). Isoscapes: Spatial pattern in isotopic biogeochemistry. *Annual Review of Earth and Planetary Sciences*, *38*(1), 161–187. https://doi.org/10.1146/annurev-earth-040809-152429

Burkhardt, S., Riebesell, U., & Zondervan, I. (1999). Effects of growth rate, CO_2 concentration, and cell size on the stable carbon isotope fractionation in marine phytoplankton. *Geochimica et Cosmochimica Acta*, *63*(22), 3729–3741. https://doi.org/10.1016/S0016-7037(99)00217-3

Chavez, F. P., Strutton, P. G., Friederich, G. E., Feely, R. A., Feldman, G. C., Foley, D. G., & McPhaden, M. J. (1999). Biological and chemical response of the equatorial Pacific Ocean to the 1997–98 El Niño. *Science*, *286*(5447), 2126–2131. https://doi.org/10.1126/science.286.5447.2126

Chiba, S., Sugisaki, H., Kuwata, A., Tadokoro, K., Kobari, T., Yamaguchi, A., & Mackas, D. L. (2012). Pan-North Pacific comparison of long-term variation in *Neocalanus* copepods based on stable isotope analysis. *Progress in Oceanography*, *97–100*, 63–75. https://doi.org/10.1016/j.pocean.2011.11.007

Crawford, W. R., & Peña, M. A. (2016). Decadal trends in oxygen concentration in subsurface waters of the Northeast Pacific Ocean. *Atmosphere-Ocean*, *54*(2), 171–192. https://doi.org/10.1080/07055900.2016.1158145

Dagg, M. J., Liu, H., & Thomas, A. C. (2006). Effects of mesoscale phytoplankton variability on the copepods *Neocalanus flemingeri* and *N. plumchrus* in the coastal Gulf of Alaska. *Deep Sea Research Part I: Oceanographic Research Papers*, *53*(2), 321–332. https://doi.org/10.1016/j.dsr.2005.09.013

de Boyer Montégut, C., Madec, G., Fischer, A. S., Lazar, A., & Iudicone, D. (2004). Mixed layer depth over the global ocean: An examination of profile data and a profile-based climatology. *Journal of Geophysical Research*, *109*(C12), C12003. https://doi.org/10.1029/2004jc002378

Dickman, E. M., Newell, J. M., González, M. J., & Vanni, M. J. (2008). Light, nutrients, and food-chain length constrain planktonic energy transfer efficiency across multiple trophic levels. *Proceedings of the National Academy of Sciences USA*, *105*(47), 18408–18412. https://doi.org/10.1073/pnas.0805566105

El-Sabaawi, R. W., Trudel, M., Mackas, D. L., Dower, J. F., & Mazumder, A. (2012). Interannual variability in bottom-up processes in

the upstream range of the California Current system: An isotopic approach. *Progress in Oceanography*, *106*, 16–27. https://doi.org/10.1016/j.pocean.2012.06.004

Espinasse, B., Hunt, B. P. V., Doson Coll, Y., & Pakhomov, E. A. (2018). Investigating high seas foraging conditions for salmon in the North Pacific: Insights from a 100 year scale archive for Rivers Inlet sockeye salmon. *Canadian Journal of Fisheries and Aquatic Sciences*, *76*, 918–927. https://doi.org/10.1139/cjfas-2018-0010

Finney, B. P., Gregory-Eaves, I., Sweetman, J., Douglas, M. S. V., & Smol, J. P. (2000). Impacts of climatic change and fishing on Pacific salmon abundance over the past 300 years. *Science*, *290*(5492), 795–799. https://doi.org/10.1126/science.290.5492.795

Fortin, M. J., & Dale, M. R. T. (2005). *Spatial analysis: A guide for ecologist*. Cambridge: Cambridge University Press.

Goldblatt, R. H., Mackas, D. L., & Lewis, A. G. (1999). Mesozooplankton community characteristics in the NE subarctic Pacific. *Deep Sea Research Part II: Topical Studies in Oceanography*, *46*(11), 2619–2644. https://doi.org/10.1016/S0967-0645(99)00078-8

Graeve, M., Albers, C., & Kattner, G. (2005). Assimilation and biosynthesis of lipids in Arctic *Calanus* species based on feeding experiments with a ^{13}C labelled diatom. *Journal of Experimental Marine Biology and Ecology*, *317*(1), 109–125. https://doi.org/10.1016/j.jembe.2004.11.016

Gruber, N., Keeling, C. D., Bacastow, R. B., Guenther, P. R., Lueker, T. J., Wahlen, M., … Stocker, T. F. (1999). Spatiotemporal patterns of carbon-13 in the global surface oceans and the oceanic suess effect. *Global Biogeochemical Cycles*, *13*(2), 307–335. https://doi.org/10.1029/1999GB900019

Hare, S. R., & Mantua, N. J. (2000). Empirical evidence for North Pacific regime shifts in 1977 and 1989. *Progress in Oceanography*, *47*(2–4), 103–145. https://doi.org/10.1016/S0079-6611(00)00033-1

Henson, S. A., & Thomas, A. C. (2008). A census of oceanic anticyclonic eddies in the Gulf of Alaska. *Deep Sea Research Part I: Oceanographic Research Papers*, *55*(2), 163–176. https://doi.org/10.1016/j.dsr.2007.11.005

Hobson, K. A. (1999). Tracing origins and migration of wildlife using stable isotopes: A review. *Oecologia*, *120*(3), 314–326. https://doi.org/10.1007/s004420050865

Horii, S., Takahashi, K., Shiozaki, T., Hashihama, F., & Furuya, K. (2018). Stable isotopic evidence for the differential contribution of diazotrophs to the epipelagic grazing food chain in the mid-Pacific Ocean. *Global Ecology and Biogeography*, *27*(12), 1467–1480. https://doi.org/10.1111/geb.12823

Hosoda, S., Ohira, T., Sato, K., & Suga, T. (2010). Improved description of global mixed-layer depth using Argo profiling floats. *Journal of Oceanography*, *66*(6), 773–787. https://doi.org/10.1007/s10872-010-0063-3

Jaeger, A., Lecomte, V. J., Weimerskirch, H., Richard, P., & Cherel, Y. (2010). Seabird satellite tracking validates the use of latitudinal isoscapes to depict predators' foraging areas in the Southern Ocean. *Rapid Communications in Mass Spectrometry*, *24*(23), 3456–3460. https://doi.org/10.1002/rcm.4792

Jennings, S., & Warr, K. J. (2003). Environmental correlates of large-scale spatial variation in the δ^{15}N of marine animals. *Marine Biology*, *142*(6), 1131–1140. https://doi.org/10.1007/s00227-003-1020-0

Karsh, K. L., Trull, T. W., Lourey, M. J., & Sigman, D. M. (2003). Relationship of nitrogen isotope fractionation to phytoplankton size and iron availability during the Southern Ocean Iron RElease Experiment (SOIREE). *Limnology and Oceanography*, *48*(3), 1058–1068. https://doi.org/10.4319/lo.2003.48.3.1058

Kline, T. C. Jr. (2009). Characterization of carbon and nitrogen stable isotope gradients in the northern Gulf of Alaska using terminal feed stage copepodite-V *Neocalanus cristatus*. *Deep Sea Research Part II: Topical Studies in Oceanography*, *56*(24), 2537–2552. https://doi.org/10.1016/j.dsr2.2009.03.004

Kurle, C. M., & McWhorter, J. K. (2017). Spatial and temporal variability within marine isoscapes: Implications for interpreting stable isotope data from marine systems. *Marine Ecology Progress Series*, *568*, 31–45. https://doi.org/10.3354/meps12045

Lalli, C. M., & Parsons, T. R. (1997). Chapter 3—Phytoplankton and primary production. In C. M. Lalli & T. R. Parsons (Eds.), *Biological oceanography: An introduction* (2nd ed., pp. 39–73). Oxford, UK: Butterworth-Heinemann.

Mackas, D. L., & Coyle, K. O. (2005). Shelf–offshore exchange processes, and their effects on mesozooplankton biomass and community composition patterns in the northeast Pacific. *Deep Sea Research Part II: Topical Studies in Oceanography*, *52*(5), 707–725. https://doi.org/10.1016/j.dsr2.2004.12.020

Mackas, D. L., & Galbraith, M. D. (2002). Zooplankton distribution and dynamics in a North Pacific eddy of coastal origin: I. Transport and loss of continental margin species. *Journal of Oceanography*, *58*(5), 725–738. https://doi.org/10.1023/a:1022802625242

Mackas, D. L., Tsurumi, M., Galbraith, M. D., & Yelland, D. R. (2005). Zooplankton distribution and dynamics in a North Pacific Eddy of coastal origin: II. Mechanisms of eddy colonization by and retention of offshore species. *Deep Sea Research Part II: Topical Studies in Oceanography*, *52*(7–8), 1011–1035. https://doi.org/10.1016/j.dsr2.2005.02.008

MacKenzie, K. M., Longmore, C., Preece, C., Lucas, C. H., & Trueman, C. N. (2014). Testing the long-term stability of marine isoscapes in shelf seas using jellyfish tissues. *Biogeochemistry*, *121*(2), 441–454. https://doi.org/10.1007/s10533-014-0011-1

MacKenzie, K. M., Palmer, M. R., Moore, A., Ibbotson, A. T., Beaumont, W. R. C., Poulter, D. J. S., & Trueman, C. N. (2011). Locations of marine animals revealed by carbon isotopes. *Scientific Reports*, *1*, 21. https://doi.org/10.1038/srep00021.

Magozzi, S., Yool, A., Vander Zanden, H. B., Wunder, M. B., & Trueman, C. N. (2017). Using ocean models to predict spatial and temporal variation in marine carbon isotopes. *Ecosphere*, *8*(5), e01763. https://doi.org/10.1002/ecs2.1763

McCutchan, J. H. Jr., Lewis, W. M. Jr., Kendall, C., & McGrath, C. C. (2003). Variation in trophic shift for stable isotope ratios of carbon, nitrogen, and sulfur. *Oikos*, *102*(2), 378–390. https://doi.org/10.1034/j.1600-0706.2003.12098.x

McMahon, K. W., Hamady, L. L., & Thorrold, S. R. (2013). *Oceanography and marine biology: An annual review* (Vol. 51, pp. 327–374). CRC Press-Taylor & Francis Group.

Merchant, C. J., Embury, O., Roberts-Jones, J., Fiedler, E., Bulgin, C. E., Corlett, G. K., … Donlon, C. (2014). Sea surface temperature datasets for climate applications from Phase 1 of the European Space Agency Climate Change Initiative (SST CCI). *Goescience Data Journal*, *1*(2), 179–191. https://doi.org/10.1002/gdj3.20

Montoya, J. P. (2008). Natural abundance of ^{15}N in Marine planktonic ecosystems. Chaper 7. In R. Michener & K. Lajtha (Eds.), *Stable isotopes in ecology and environmental science*. Wiley. https://doi.org/10.1002/9780470691854.ch7

Montoya, J. P., Carpenter, E. J., & Capone, D. G. (2002). Nitrogen fixation and nitrogen isotope abundances in zooplankton of the oligotrophic North Atlantic. *Limnology and Oceanography*, *47*(6), 1617–1628. https://doi.org/10.4319/lo.2002.47.6.1617

Montoya, J. P., & McCarthy, J. J. (1995). Isotopic fractionation during nitrate uptake by phytoplankton grown in continuous culture. *Journal of Plankton Research*, *17*(3), 439–464. https://doi.org/10.1093/plankt/17.3.439

Needoba, J. A., Foster, R. A., Sakamoto, C., Zehr, J. P., & Johnson, K. S. (2007). Nitrogen fixation by unicellular diazotrophic cyanobacteria in the temperate oligotrophic North Pacific Ocean. *Limnology and Oceanography*, *52*(4), 1317–1327. https://doi.org/10.4319/lo.2007.52.4.1317

Peña, M. A., Nemcek, N., & Robert, M. (2018). Phytoplankton responses to the 2014–2016 warming anomaly in the northeast subarctic Pacific Ocean. *Limnology and Oceanography*, *64*(2), 515–525. https://doi.org/10.1002/lno.11056

Pennock, J. R., Velinsky, D. J., Ludlam, J. M., Sharp, J. H., & Fogel, M. L. (1996). Isotopic fractionation of ammonium and nitrate during uptake by *Skeletonema costatum*: Implications for $\delta^{15}N$ dynamics under bloom conditions. *Limnology and Oceanography*, *41*(3), 451–459. https://doi.org/10.4319/lo.1996.41.3.0451

Pethybridge, H., Choy, C. A., Logan, J. M., Allain, V., Lorrain, A., Bodin, N., … Olson, R. J. (2018). A global meta-analysis of marine predator nitrogen stable isotopes: Relationships between trophic structure and environmental conditions. *Global Ecology and Biogeography*, *27*(9), 1043–1055. https://doi.org/10.1111/geb.12763

Post, D. M. (2002). Using stable isotopes to estimate trophic position: Models, methods, and assumptions. *Ecology*, *83*(3), 703–718. https://doi.org/10.2307/3071875

R Core Team. (2018). *R: A language and environment for statistical computing*. Vienne, Austria: R Foundation for Statistical Computing. Retrieved from http://www.R-project.org/

Rolff, C. (2000). Seasonal variation in $\delta^{13}C$ and $\delta^{15}N$ of size-fractionated plankton at a coastal station in the northern Baltic proper. *Marine Ecology Progress Series*, *203*, 47–65. https://doi.org/10.3354/meps203047

Smyntek, P. M., Teece, M. A., Schulz, K. L., & Thackeray, S. J. (2007). A standard protocol for stable isotope analysis of zooplankton in aquatic food web research using mass balance correction models. *Limnology and Oceanography*, *52*(5), 2135–2146. https://doi.org/10.4319/lo.2007.52.5.2135

Somes, C. J., Schmittner, A., Galbraith, E. D., Lehmann, M. F., Altabet, M. A., Montoya, J. P., … Eby, M. (2010). Simulating the global distribution of nitrogen isotopes in the ocean. *Global Biogeochemical Cycles*, *24*(4), 1–16. https://doi.org/10.1029/2009GB003767

Sousa, L., Coyle, K. O., Barry, R. P., Weingartner, T. J., & Hopcroft, R. R. (2016). Climate-related variability in abundance of mesozooplankton in the northern Gulf of Alaska 1998–2009. *Deep Sea Research Part II: Topical Studies in Oceanography*, *132*, 122–135. https://doi.org/10.1016/j.dsr2.2016.04.006

St. John Glew, K., Graham, L. J., McGill, R. A. R., & Trueman, C. N. (2019). Spatial models of carbon, nitrogen and sulphur stable isotope distributions (isoscapes) across a shelf sea: An INLA approach. *Methods in Ecology and Evolution*, *10*(4), 518–531. https://doi.org/10.1111/2041-210X.13138

Tiselius, P., & Fransson, K. (2016). Daily changes in $\delta^{15}N$ and $\delta^{13}C$ stable isotopes in copepods: Equilibrium dynamics and variations of trophic level in the field. *Journal of Plankton Research*, *38*(3), 751–761. https://doi.org/10.1093/plankt/fbv048

Trueman, C. N., MacKenzie, K. M., & Glew, K. S. J. (2017). Stable isotope-based location in a shelf sea setting: Accuracy and precision are comparable to light-based location methods. *Methods in Ecology and Evolution*, *8*(2), 232–240. https://doi.org/10.1111/2041-210X.12651

Trueman, C. N., MacKenzie, K. M., & Palmer, M. R. (2012). Identifying migrations in marine fishes through stable-isotope analysis. *Journal of Fish Biology*, *81*(2), 826–847. https://doi.org/10.1111/j.1095-8649.2012.03361.x

Vander Zanden, H. B., Tucker, A. D., Hart, K. M., Lamont, M. M., Fujisaki, I., Addison, D. S., … Bjorndal, K. A. (2015). Determining origin in a migratory marine vertebrate: A novel method to integrate stable isotopes and satellite tracking. *Ecological Applications*, *25*(2), 320–335. https://doi.org/10.1890/14-0581.1

Whitney, F. A. (2015). Anomalous winter winds decrease 2014 transition zone productivity in the NE Pacific. *Geophysical Research Letters*, *42*(2), 428–431. https://doi.org/10.1002/2014GL062634

Williams, B., Risk, M., Stone, R., Sinclair, D., & Ghaleb, B. (2007). Oceanographic changes in the North Pacific Ocean over the past century recorded in deep-water gorgonian corals. *Marine Ecology Progress Series*, *335*, 85–94. https://doi.org/10.3354/meps335085

Williams, R. L., Wakeham, S., McKinney, R., & Wishner, K. F. (2014). Trophic ecology and vertical patterns of carbon and nitrogen stable isotopes in zooplankton from oxygen minimum zone regions. *Deep Sea Research Part I: Oceanographic Research Papers*, *90*, 36–47. https://doi.org/10.1016/j.dsr.2014.04.008

Wood, S. N. (2004). Stable and efficient multiple smoothing parameter estimation for generalized additive models. *Journal of the American Statistical Association*, *99*(467), 673–686. https://doi.org/10.1198/016214504000000980

Wood, S. N. (2011). Fast stable restricted maximum likelihood and marginal likelihood estimation of semiparametric generalized linear models. *Journal of the Royal Statistical Society: Series B (Statistical Methodology)*, *73*(1), 3–36. https://doi.org/10.1111/j.1467-9868.2010.00749.x

Wunder, M. B. (2012). Determining geographic patterns of migration and dispersal using stable isotopes in keratins. *Journal of Mammalogy*, *93*(2), 360–367. https://doi.org/10.1644/11-MAMM-S-182.1

Zuur, A. F. (2012). *A beginner's guide to generalized additive models with R*. Newburgh, NY: Highland Statistics Limited.

Zuur, A. F., Ieno, E. N., & Elphick, C. S. (2010). A protocol for data exploration to avoid common statistical problems. *Methods in Ecology and Evolution*, *1*(1), 3–14. https://doi.org/10.1111/j.2041-210X.2009.00001.x

BIOSKETCH

Boris Espinasse is interested in biophysical interactions, zooplankton ecology and trophic interactions in marine ecosystems. He uses stable isotopes as a tool to obtain information on these primordial aspects of ecosystem dynamics. More information about him can be found at: https://www.researchgate.net/profile/Boris_Espinasse

SUPPORTING INFORMATION

Additional supporting information may be found online in the Supporting Information section.

How to cite this article: Espinasse B, Hunt BPV, Batten SD, Pakhomov EA. Defining isoscapes in the Northeast Pacific as an index of ocean productivity. *Global Ecol Biogeogr.* 2019;00:1–16. https://doi.org/10.1111/geb.13022